

# BRIGHT

Erasmus+ strategic partnership for Higher Education

**BOOSTING THE SCIENTIFIC EXCELLENCE AND  
INNOVATION CAPACITY OF 3D PRINTING METHODS  
IN PANDEMIC PERIOD**

## TOOLKIT 2

**DESIGN AND SLM MANUFACTURING  
OF CUSTOM FACIAL IMPLANT USED  
TO RECONSTRUCT THE  
SUPRAORBITAL MARGIN AND  
ZYGOMATIC BONE.**

<b>Project Title</b>	<b>Boosting the scientific excellence and innovation capacity of 3D printing methods in pandemic period 2020-1-RO01-KA226-HE-095517</b>
<b>Output</b>	<b>IO2 – BRIGHT e-toolkit manual for digital learning in producing medical parts by 3D printing methods in the context of the pandemic</b>
<b>Toolkit</b>	<b>Toolkit 2 Selective laser melting</b>
<b>Date of Delivery</b>	<b>November 2021</b>
<b>Authors</b>	<b>Cosmin COSMA, Petru BERCE, Nicolae Balc</b>
<b>Version</b>	<b>Final variant</b>

## Contents

1. Introduction .....	3
2. Theoretical background.....	4
2.1 Realizer 250 equipment and working principle.....	4
2.2 SLM Realizer 250 machine .....	5
2.3 Powders for SLM process .....	6
2.4 Conventional plates used in maxillofacial surgery.....	7
2.5 Frequent risk of fracture .....	8
3. Work methodology.....	9
3.1 CT reconstruction .....	9
3.2 Implant design .....	12
3.3 Pre-processing .....	15
3.4. Configure the SLM process parameters .....	18
3.5 SLM simulation .....	21
3.6 Estimation of production time and cost.....	22
3.7 SLM-manufacturing of implant.....	23

This project has been funded with support from the European Commission. This publication [communication] reflects the views only of the authors, and the Commission cannot be held responsible for any use which may be made of the information contained therein.

## 1. Introduction

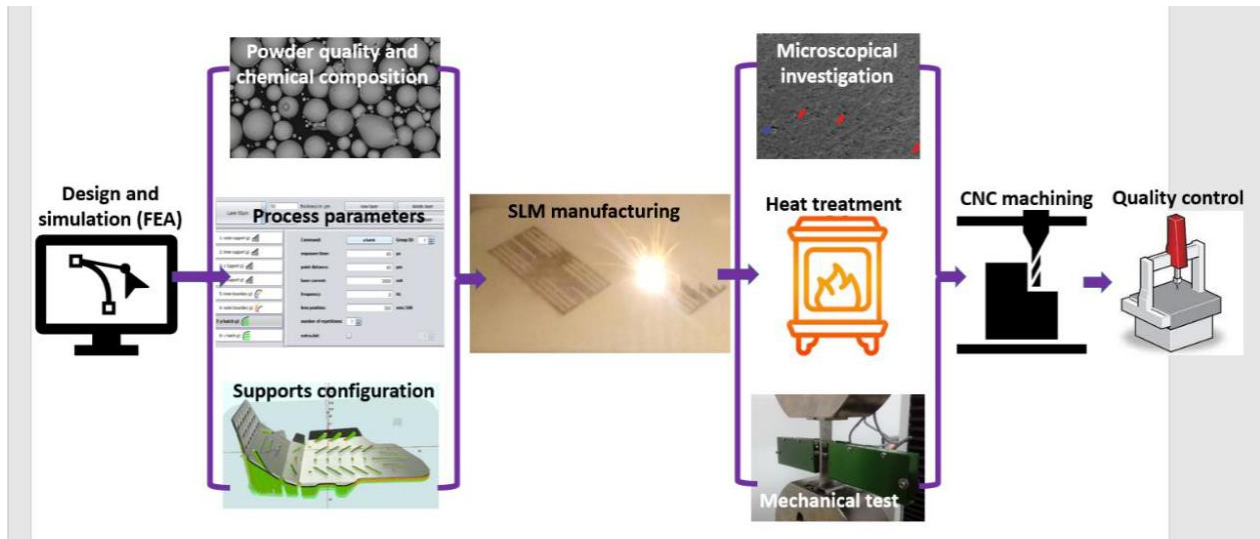
Over the last two decades, the concept of product customization has received increased attention from both academia and industry. Recent developments in digital fabrication technologies have made product personalization not only technically doable but also economically profitable [Pradel]. Selective laser melting (SLM) is capable to fabricate directly custom products. In healthcare, product customization is already an established practice using SLM technology. In this domain, cost considerations are less prominent and personalized components provide incomparable advantages. The basic component of SLM systems is the Nd:YAG laser, which emits continuous light in the infrared spectrum with a wavelength of 1064 nm. SLM process is capable to produce metallic parts with 99.9% relative density. Most of the SLM research were developed using the following powders as stainless steel, pure titanium, titanium alloy (Ti6Al4V), Co-Cr, and nickel (Inconel 625, Inconel 718) [Yap], [Lietaert], [Leordean], [Fateri]. The ongoing transition to digital manufacturing prompts new possibilities of SLM process. The main benefits of SLM parts include [Aniwa]:

- **It is possible to fabricate complex components** that would have to be broken down into several pieces with conventional methods (examples casting or CNC milling).
- Compared to CNC milling or turning, **SLM manufacturing produces less waste** as it only consumes the material needed for a certain part. Moreover, it is possible to re-use the un-melted powder.

In the last years, custom SLM implants were developed to treat total knee arthroplasty [Murr], chondrosarcoma localized in calcaneum [Imanishi], and maxillofacial reconstructions [Rotaru], [Parthasarathy], [Armencea]. The results of these pilot surgical interventions are acceptable, the SLM implants being integrated into the body without any signs of rejection and improving patients' health.

## 2. Theoretical background

### SLM WORKFLOW



#### 2.1 Realizer 250 equipment and working principle

Founded by Dr. Matthias Fockele, one of the two physicists that developed and patented the SLM (Figure 2.1), Realizer company was one of the leading producers of SLM machines. In 1999, the company delivered the world's first SLM machine for metals at the research centre in Karlsruhe [Realizer]. DMG Mori announced the acquisition of the majority Realizer stake (50.1%) in 2017 [Sher].

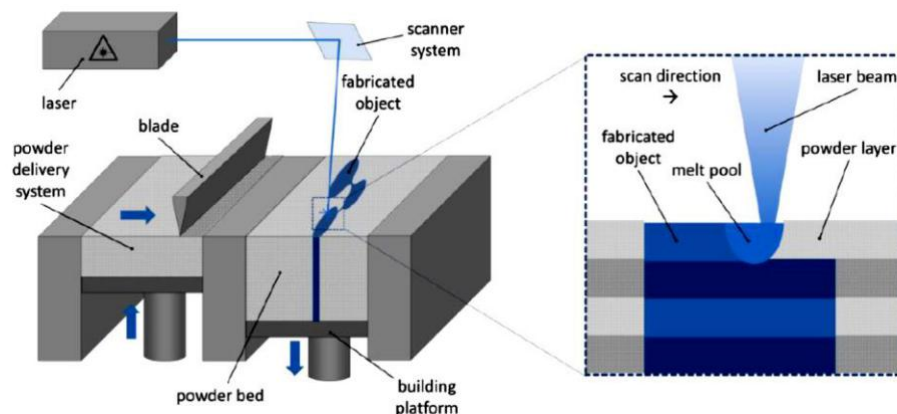


Fig. 2.1. Working principle of SLM. Source: [www.realizer.com](http://www.realizer.com)

This project has been funded with support from the European Commission. This publication [communication] reflects the views only of the authors, and the Commission cannot be held responsible for any use which may be made of the information contained therein.

## 2.2 SLM Realizer 250 machine

TUCN additive manufacturing lab buy in 2008 a SLM Realizer 250 machine (Germany). This SLM machine costs 0.5 mil. € and under slice-by-slice principle is capable to produce customized implants. The machine is equipped with a 200 W solid fiber laser (type Nd:YAG) and emits continuous light in the infrared spectrum with a wavelength of 1064 nm. The main technical characteristics are presented in Figure 2.2. Other technical data are as following:  $\pm 0.10$  mm dimensional accuracy, 50  $\mu\text{m}$  common layer thickness, less than 0.5% internal porosity, always required supports, inert gas argon or nitrogen depends on power type, heated platform up to 250°C, typical surface roughness Ra between 8  $\mu\text{m}$  to 10  $\mu\text{m}$ , and 100-1500 mm/s scanning speed.

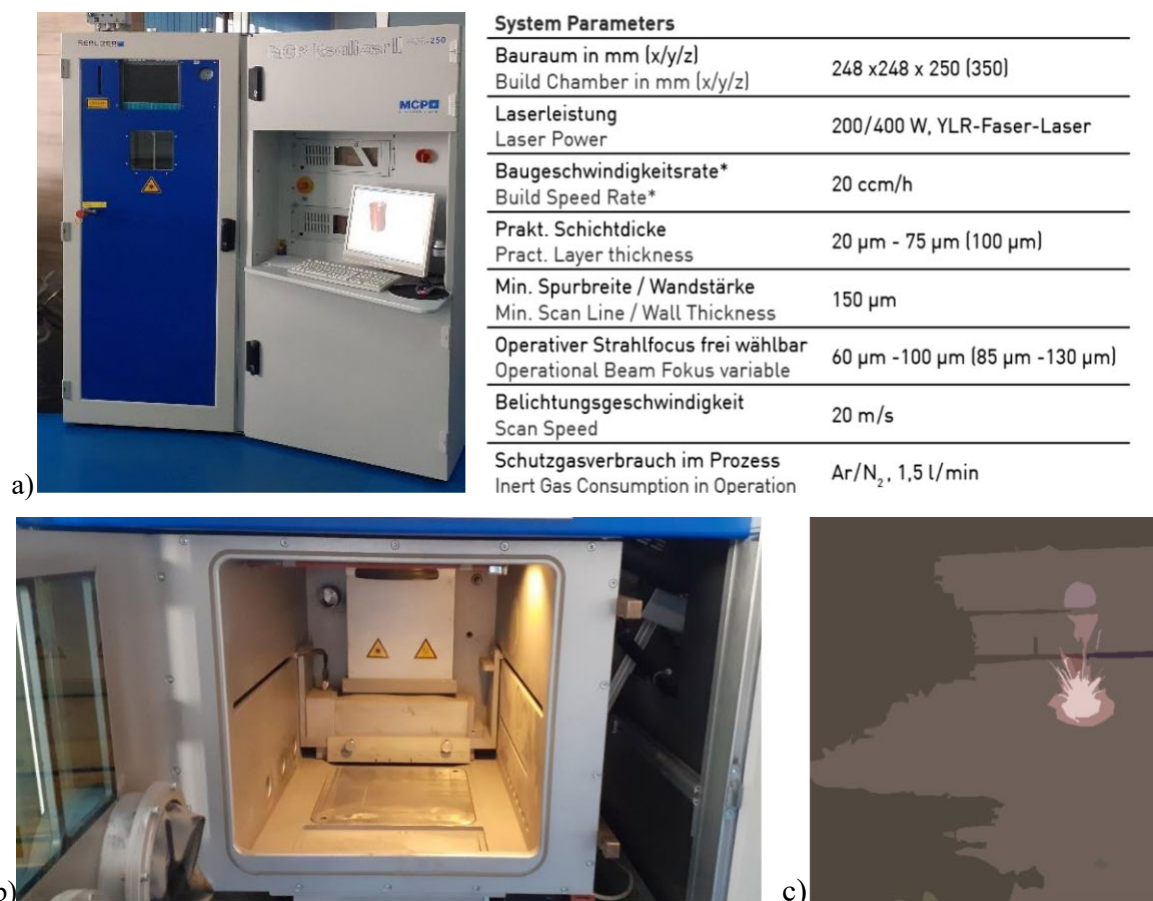


Fig. 2.2. SLM Realizer 250 machine: a) Technical data, b) Manufacturing chamber, c) Graphical animation of laser scanning

This project has been funded with support from the European Commission. This publication [communication] reflects the views only of the authors, and the Commission cannot be held responsible for any use which may be made of the information contained therein.

### 2.3 Powders for SLM process

Generally, this machine works with the following gas atomized powders as tool steel and stainless steel, pure titanium (Ti), titanium alloy (Ti6Al4V), Co-Cr, aluminum, and nickel (Inconel 625, 718). Information about particles shape and size are essential in controlling the SLM process. The shape of grains is spherical and have a diameter between 10  $\mu\text{m}$  to 90  $\mu\text{m}$  (Figure 2.3). The particle size distribution is described in percentiles, common is offer d90 value. This d-value indicate that 90% of particles are finer than this diameter according to laser diffraction result. It was observed that d90 value for normal SLM powder ranging from 20  $\mu\text{m}$  to 60  $\mu\text{m}$ . Moreover, the particle flowability can be measured using a hall flowmeter funnel with an orifice of 2.5 mm and is possible to calculate the flow rate (s/50g). The hall flow rate is expressed as the time required for a 50 g powder sample to be discharged by gravitational force through the flowmeter funnel (ASTM B213). Typical flow rate is between 15s to 40s per 50g of powder.

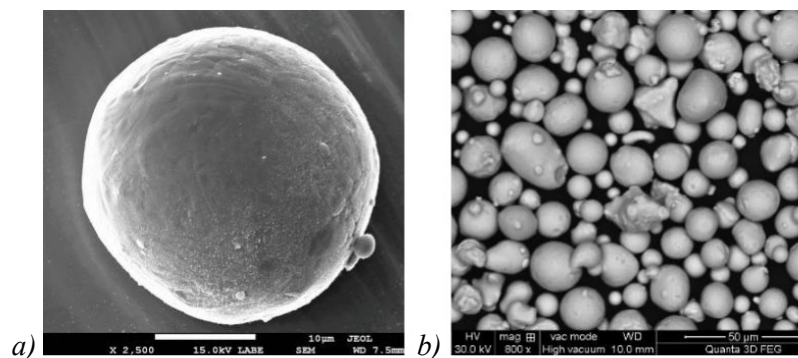


Fig. 2.3. SLM powders: a) Co-Cr alloy, b) pure Titanium

Some of the most representative powder makers are as following: Bego, Carpenter Additive, CNPC Powder, Fehrmann Alloys, GE Additive, Höganäs, Metalpine, Mimete, Oerlikon Additive, Osaka Titanium Techn., Safina, Sandvik Osprey, and Scheftner Dental Alloys. The below listed prices are just indications for biocompatible powders.

Titanium Alloy TiAl6V4:	420 – 540 €/kg
Pure Titanium Grade 1 or 2:	360 – 480 €/kg
Stainless Steel 316L (1.4404):	70 – 110 €/kg
Cobalt Chromium Alloy (CoCrWMo):	240 – 370 €/kg

This project has been funded with support from the European Commission. This publication [communication] reflects the views only of the authors, and the Commission cannot be held responsible for any use which may be made of the information contained therein.

## 2.4 Conventional plates used in maxillofacial surgery

The technological evolution has greatly contributed to the modernization of the medical field, through the improvement of the quality of products as well as of the medical act [Cosma'2017]. This trend is triggered by an aging society, with a higher life expectancy. The implants or plates commercialized currently do not cover the multitude of medical cases that deal with individual osseous problems that appeared because of traumas, malformations, or osseous tumors. Figure 2.4 presents standard plates conventional manufactured used in maxillofacial surgery to treat simple fractures, being made of pure titanium Grade II.

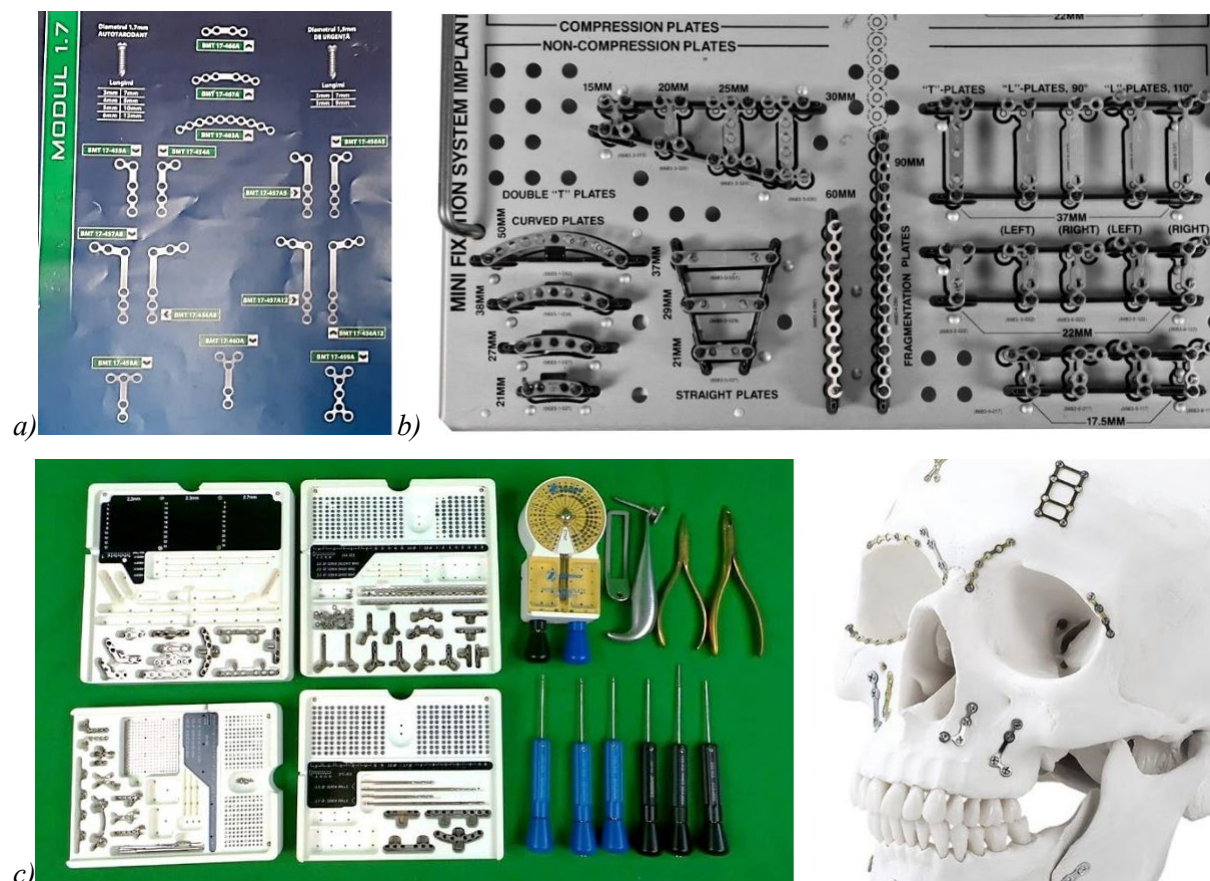


Fig. 2.4. Standard plates conventional manufactured used in maxillofacial surgery to treat fractures, being made of pure titanium, produced by: a) BioMicron Transilvania; b) Striker; c) Zimmer

This project has been funded with support from the European Commission. This publication [communication] reflects the views only of the authors, and the Commission cannot be held responsible for any use which may be made of the information contained therein.

### 2.5 Frequent risk of fracture

A recent report published by National Clinical Research Center for Oral Diseases (Shanghai, China) shows that the various fracture patterns depend on the mechanism and degree of the externally applied forces, with the usually reported causes including automobile traffic accidents (37%), work accidents (21%), bike accidents (19%), falls (13%), striking an object (7%) [Casole]. This 10-year retrospective study reveal that the most common fractured bones of facial were the zygomatic arch, nasal bone, orbital floor, zygomaticomaxillary area, and mandible bone [Casole]. The most affected patients have between 19 to 29 years old (28%) and between 30 to 39 years old (22%). In general, all the patients suffer also postinjury complications such as malocclusion, limited mouth opening, infraorbital nerve palsy, and blindness. The summary of this extended report is detailed in Figure 2.5.

Considering this report and others [Rotaru], [Parthasarathy], the present laboratory work is focused on a complex facial bone which is frequent fractured as zygomatic bone.

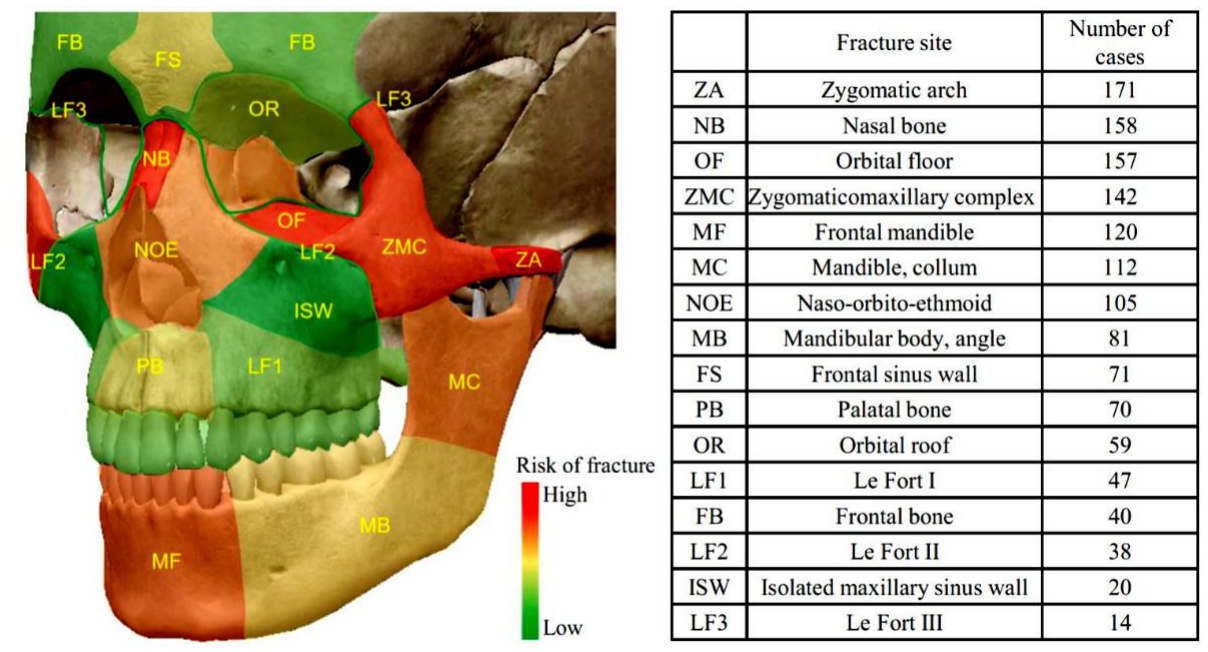


Fig.2.5 Facial skeleton showing the frequent risk of fracture [Casole]

This project has been funded with support from the European Commission. This publication [communication] reflects the views only of the authors, and the Commission cannot be held responsible for any use which may be made of the information contained therein.

### 3. Work methodology

#### 3.1 CT reconstruction

To support the surgeons in complex reconstruction cases, various studies were developed, and the method of design-manufacturing was established. Using computer tomography (CT) images is it possible to design and fabricate directly customized anatomical implants using SLM process and biocompatible alloys. The customized implants are precisely adjusted to the implant area, eliminating the restrictions of shape, reducing the length of the surgical intervention through preparatory simulations, and they can have physical-mechanical features like those manufactured through conventional technologies [Rotaru], [Parthasarathy]. All these aspects lead to the diminishment of the chances of infection or rejection by the body, as well as to the more rapid recovery of the patient.

InVesalius is public health software that performs analysis and segmentation of virtual anatomical models, enabling the creation of physical models with the aid of additive manufacturing [InVesalius]. From 2D images obtained through CT, the program allows to create 3D anatomical representations of bones (Figure 3.1). It was named in honor of the Belgian dr. Andreas Vesalius (1514-1564), widely considered the father of modern anatomy. This software was developed by Center for Information Technology Center Renato Archer. The use of visualization technologies and 3D analysis of CT images, when combined with additive manufacturing, can assist the surgeon in diagnosing, surgical planning, and simulation of complex bone defects.



Figure 3.1. InVesalius software

This project has been funded with support from the European Commission. This publication [communication] reflects the views only of the authors, and the Commission cannot be held responsible for any use which may be made of the information contained therein.

The present laboratory work is focused on a complex facial bone which is frequent fractured as zygomatic bone. Figure 3.2 details the anatomy of skull (anterior view), marking with red squares the targeted facial bones as frontal zygomatic bone, orbital surface of zygomatic bone, and supraorbital margin.

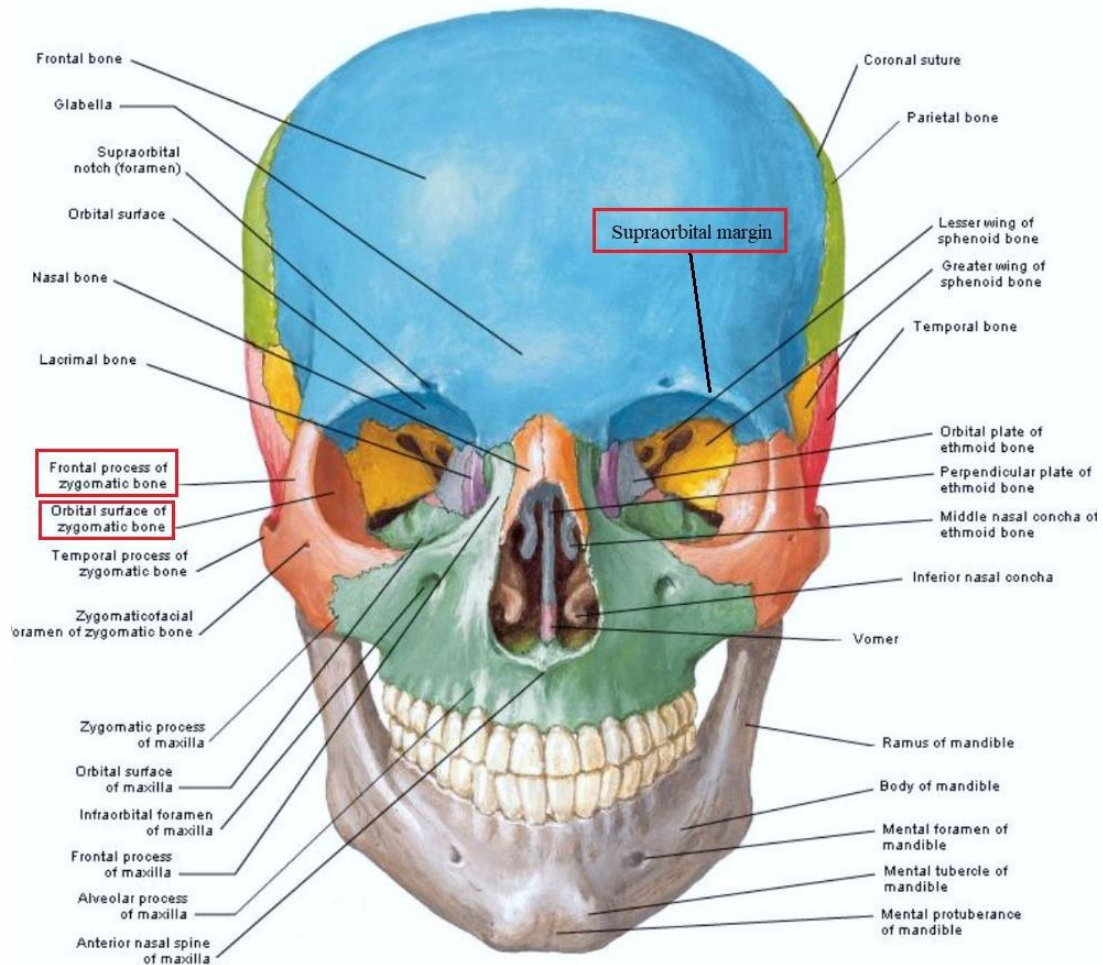
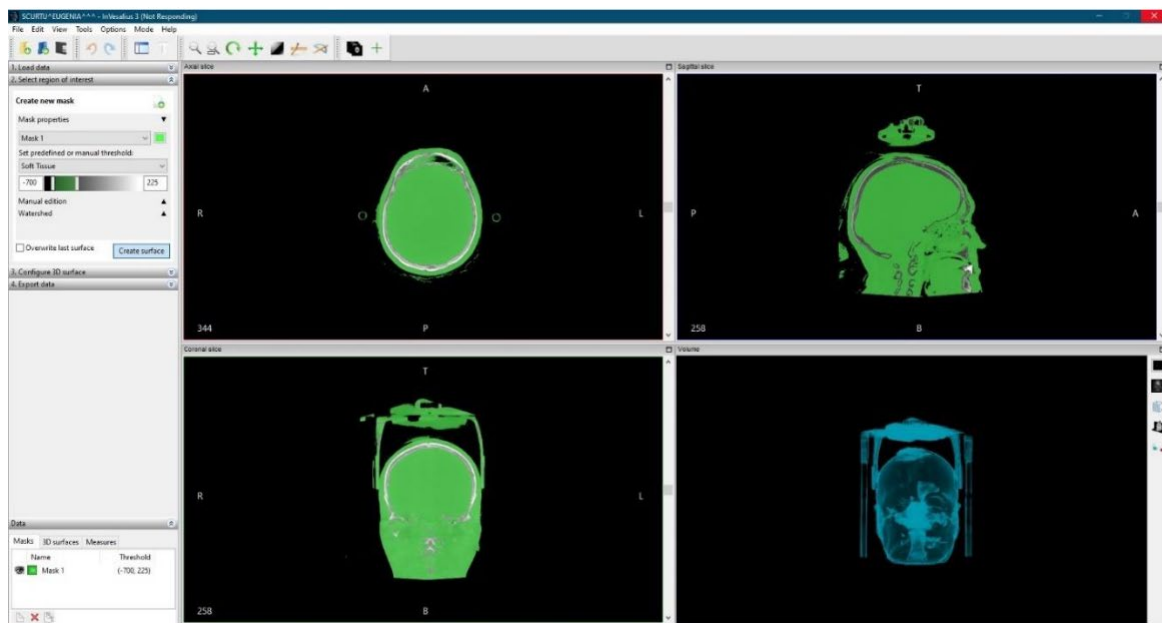
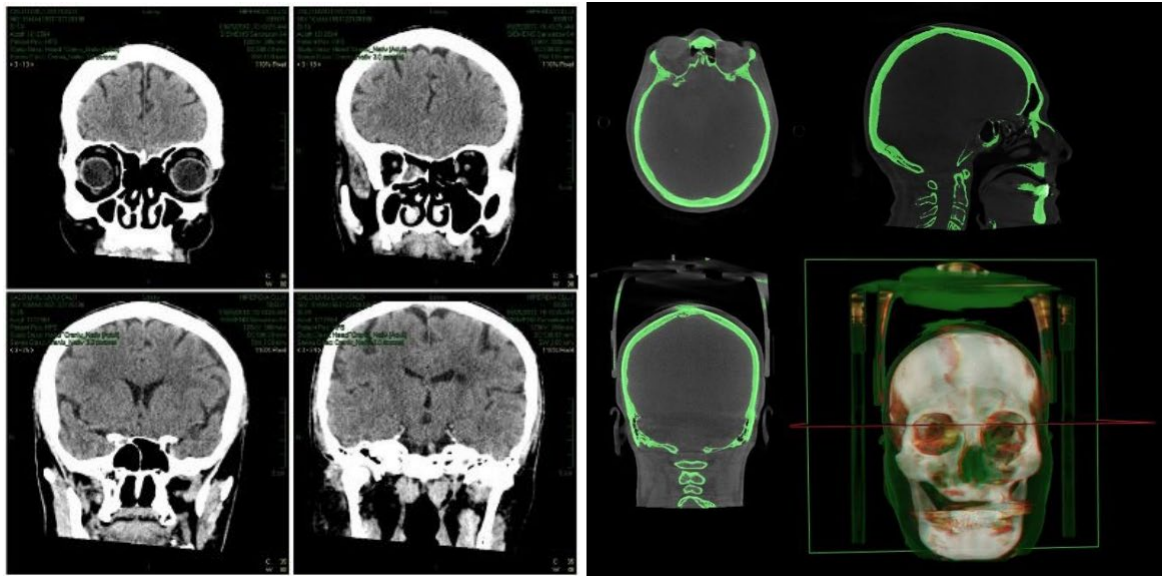


Fig. 3.2. Anatomy of facial bones [Chung]

In this work, we used CT images of a 69-year-old female who volunteered for us to reconstruct 3D models. The CT images were taken with a Promax scanner (Planmeca, Finland). The following scan parameters were used: 88 kV, 7 mA, 0.2 mm layer thickness, 400 slices, and 12 s exposure time. Using the CT images, the surgeons could establish the diagnosis and

This project has been funded with support from the European Commission. This publication [communication] reflects the views only of the authors, and the Commission cannot be held responsible for any use which may be made of the information contained therein.

suggest a treatment method [Armencea]. The DICOM images were imported in InVesalius software for medical data processing and adjustments (Figure 3.3 and Figure 3.4).



*Fig. 3.3. CT reconstruction of patient facial bones*

This project has been funded with support from the European Commission. This publication [communication] reflects the views only of the authors, and the Commission cannot be held responsible for any use which may be made of the information contained therein.

Figure 3.4 is showing the virtual reconstruction of facial bones and soft tissues (skin), where the defect area is marked with red color. Steps undertaken were threshold segmentation, surface generation and .STL exportation of virtual bone.

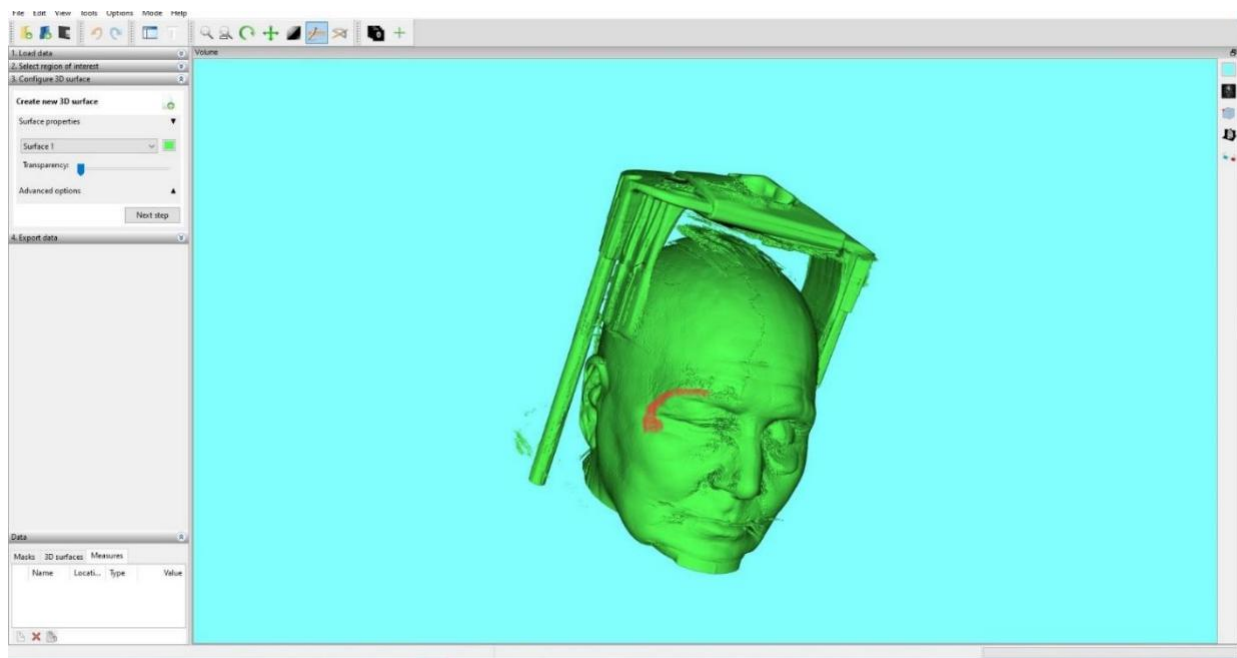


*Fig. 3.4. Virtual reconstruction of facial bones and soft tissues (skin); The defect area is marked with red color, location supraorbital margin and frontal zygomatic bone*

### **3.2 Implant design**

During the digitization and processing of CT images, we obtained the 3D mask of the targeted facial bones which were exported in .STL format. Figure 3.5 shows the virtual model of supraorbital margin and frontal zygomatic bone. This virtual reconstruction of custom implant can be used to treat a large bone defect located in supraorbital margin, frontal zygomatic bone, and its orbital surface. If the targeted area is destroyed, the initial model of implant should be created using mirror function (see Ref. [Armencea'2019]). This initial version of implant will be used as master model. To fix and repair all the errors from the virtual model (.STL file), Autodesk Meshmixer software was used. This free software is a prototype design tool based on high-resolution dynamic triangle meshes.

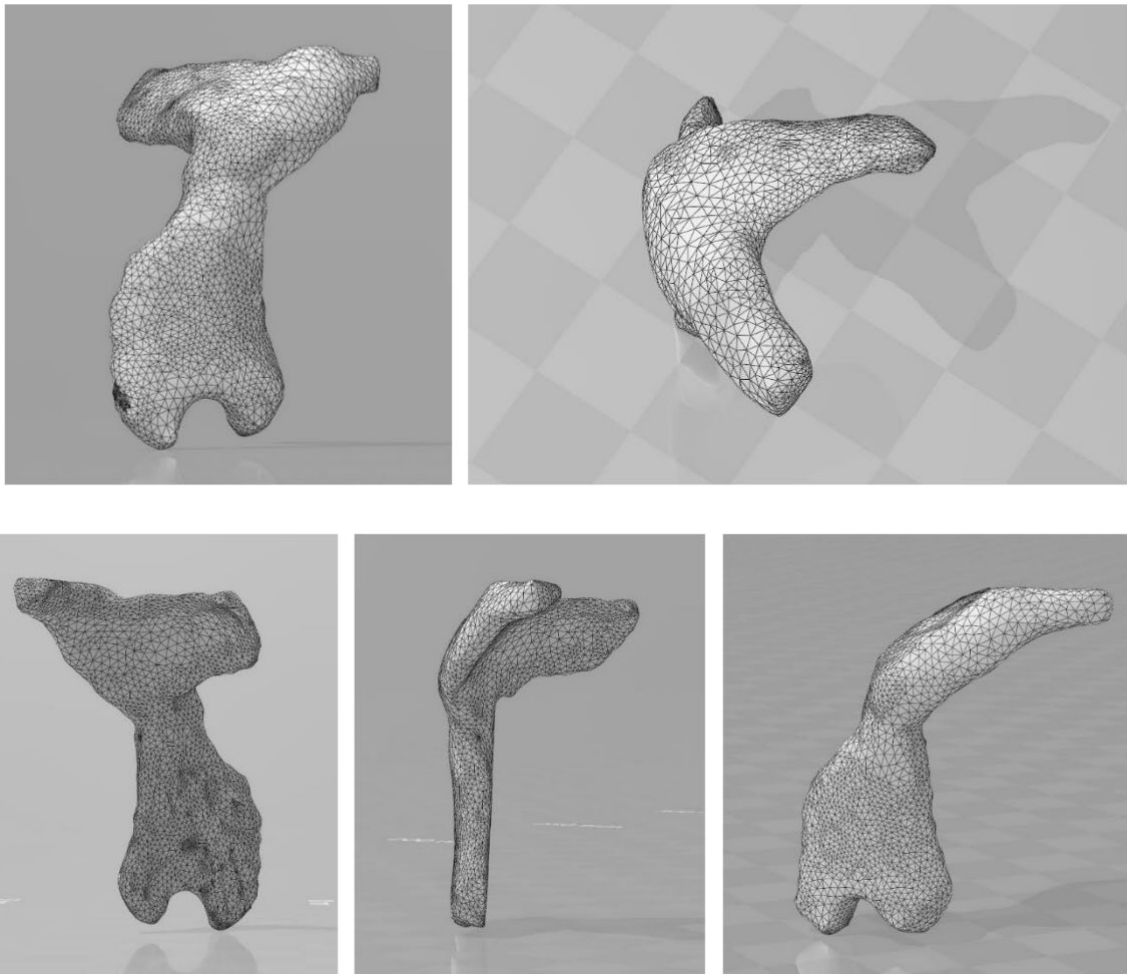


*Fig. 3.5 Initial version of facial implant (master model)*

After the implant model was clean off surface errors and defects, the model was imported in SolidWork software. Here, the implant was prepared considering two directions as following weight reduction and fixation zones. For weight reduction of implant, 32 holes with 1.1 mm diameter were used to perforate the orbital surface of zygomatic area (see Figure 3.6). For fixing the implant, 2 holes with 2.6 mm diameter were created. Taken into consideration the mechanical properties of Ti processed by SLM, advanced topological optimization and reduction of weight can be applied on this implant using finite element analysis simulations. In this way, the design of custom implant can be optimized under SolidWorks Simulations or ANSYS analysis.

This project has been funded with support from the European Commission. This publication [communication] reflects the views only of the authors, and the Commission cannot be held responsible for any use which may be made of the information contained therein.



*Fig. 3.6. Creating 2 fixing holes with 2.6 mm diameter and perforate the orbital surface of zygomatic bone with 32 holes with 1.1 mm diameter*

To improve the fixation of implant, we added a superior fixing area. Figure 3.7 presents the final design of implant. The final design of Ti implant has 2.13 cm<sup>3</sup> and 9.64 g (Figure 3.8). If is necessary, repair all the geometrical defects from STL file such as: connecting unmatched edges, closing holes, aligning triangular normal, resolving overlapping areas. After we accomplished these steps, the edges of implant surface were smoothed in Meshmixer software.

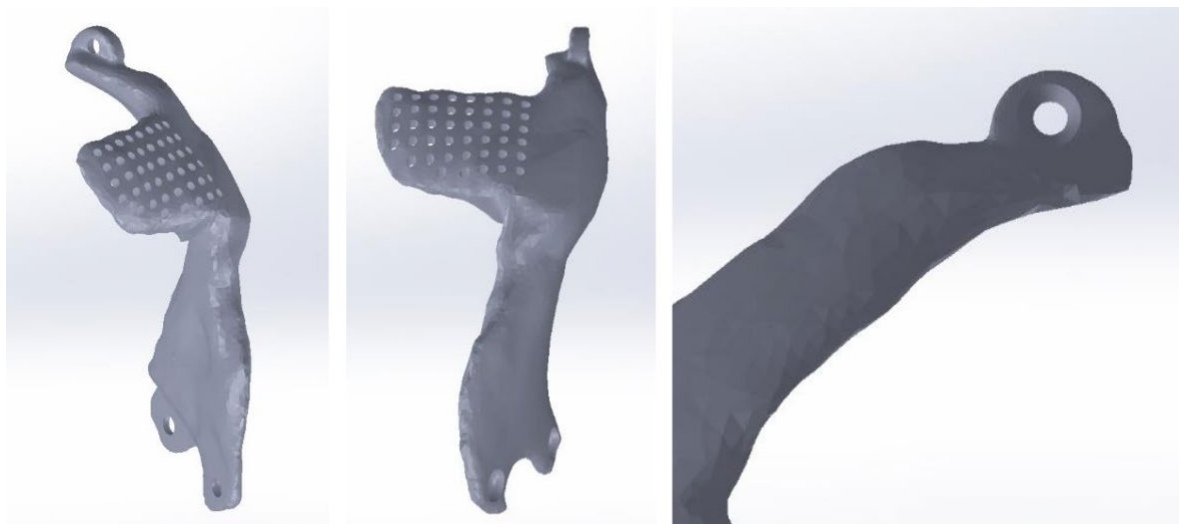


*Fig. 3.7. Final design of implant after a fixing area was added superior; In total are 3 holes for fixing the implant with screw bones*

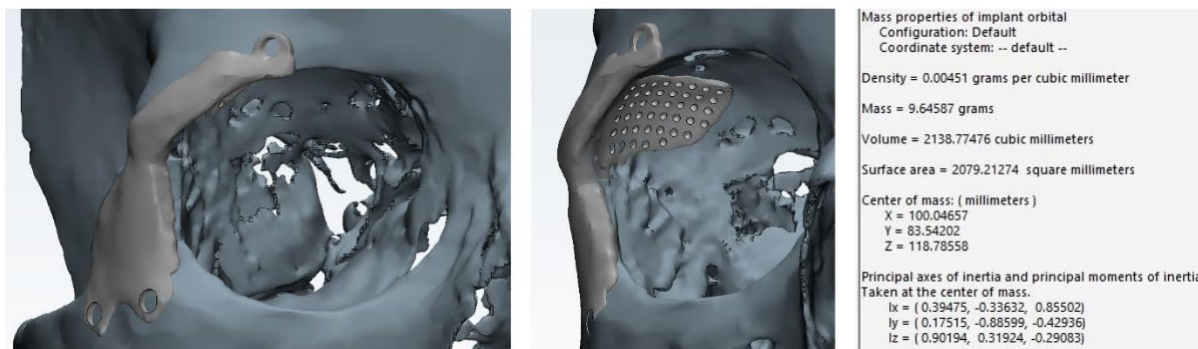


Fig. 3.8. Final design of Ti implant, weight 9.64 g, volume 2.13 cm<sup>3</sup>

The designed implant should fit perfectly to the orbit's topographic characteristics. This process enables the precise reconstruction of the defects, even when there are significant parietal fractures on both sides of the head [Avinent]. Particular focus was placed on orbit complicated geometry.

### 3.3 Pre-processing

To fabricate the implant, we will use pure Ti powder which corresponds to standard Ti Grade 1, having a purity of 99.5%. Identify and note the powder cost and the main physical-mechanical properties in Table 1. The Ti powder should have spherical granules with proper diameter for SLM printing and high biocompatibility.

Table 1. Physical-mechanical properties of Ti implants SLM-manufactured

Commercial name	Yield Tensile strength (MPa)	Ultimate Tensile strength (MPa)	Elongation or Strain (%)	Young Modulus (GPa)	Density [g/cm <sup>3</sup> ]	Hardness [HRC or HB]	Powder diameter [μm]	Supplier

Angled surfaces more than 45° are possible to be built without supports structures according to multiples experimental studies [Cosma'2019] and German Standard VDI 3405 [VDI]. A self-supporting angle describes the feature's angle relative to the build

This project has been funded with support from the European Commission. This publication [communication] reflects the views only of the authors, and the Commission cannot be held responsible for any use which may be made of the information contained therein.

platform (XY plane). A sketch of this principal is illustrated in Figure 15 where is presented a cross-section of a profile which has different  $\delta$  angles between the surfaces and the SLM plate. This sketch demonstrates the importance of building orientation on SLM plate and how we can improve the design of parts.

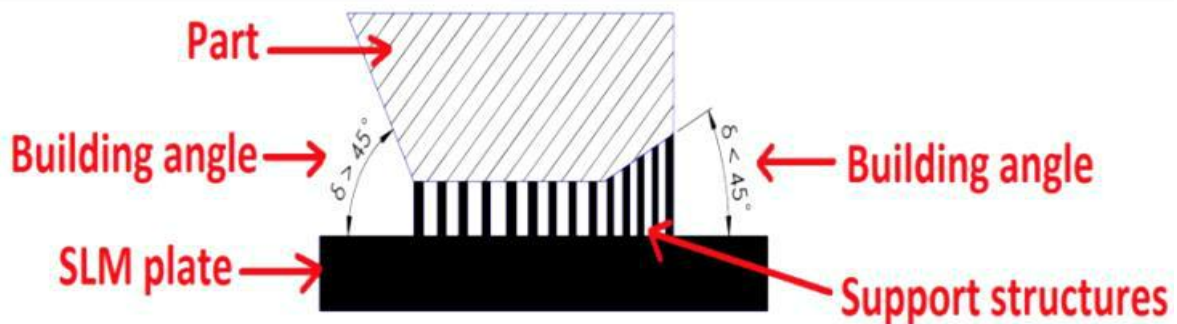


Fig. 3.9. Support structures needed to anchor surfaces. Surfaces with angles higher than  $45^\circ$  are possible to fabricate without supports [Cosma '2019]

Now, you should establish the best building orientation of implant to have a reduced production time. Use RDesigner software from Realizer machine and an example is listed in Figure 3.10. For easily removing the supports, the distance between the implant and the build platform should be 3 mm. The part orientation is a critical aspect, and it should be adapted/optimized for each model according to user needs (example: reduced build time, low surface roughness, or high mechanical resistance on a specified direction).

Also configure the proper support structures to anchor the model. Support structures are required to sustain the next layer built upon, to anchor the part on the build plate and to prevent the warping effect. RDesigner offer the possibility to model a new type of them called “lattice supports”. The lattice pattern can be configured in different ways, modifying the unit cell between 0.5 mm to 2.5 mm. This type of lattice support is illustrated in Figure 3.10.

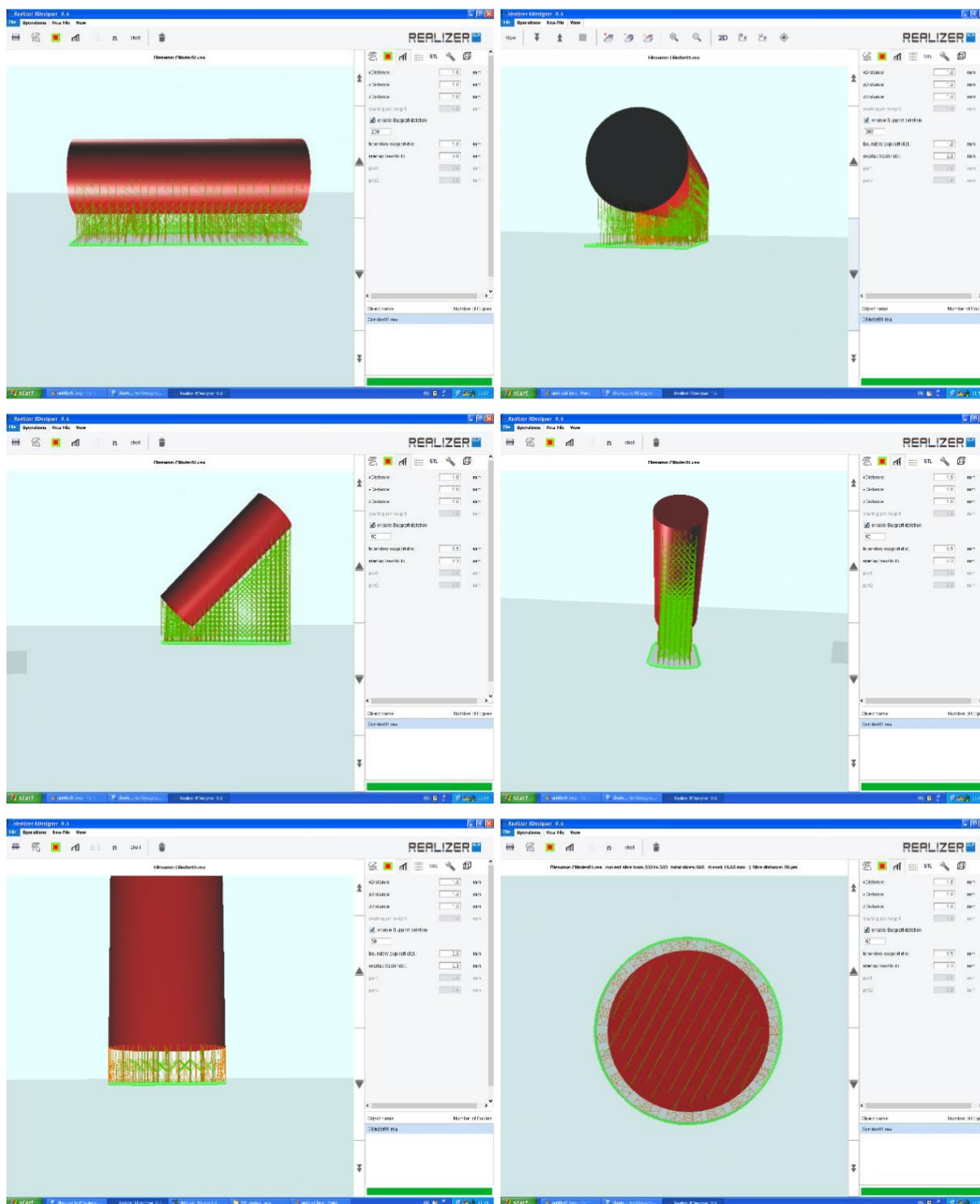
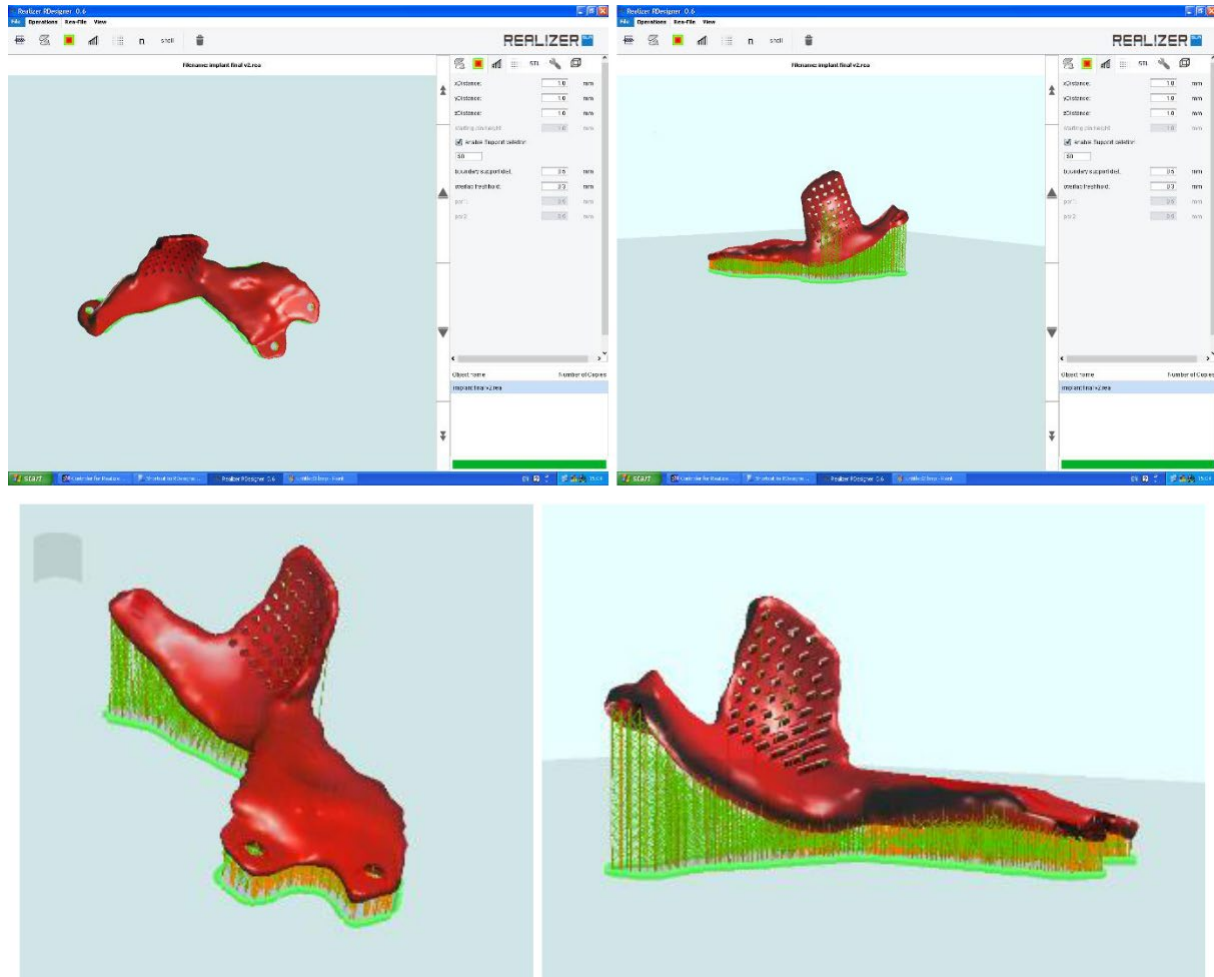


Fig. 3.10. Different building orientations of implant and its support structures, RDesigner software:  
Horizontal, angled at 45°, and vertical

This project has been funded with support from the European Commission. This publication [communication] reflects the views only of the authors, and the Commission cannot be held responsible for any use which may be made of the information contained therein.

Figure 3.11 shows the optimal building orientation of implant on SLM platform, and its support structures generated. The lattice unit of support structure was setup at  $x=y=z=1.0$  mm. These steps were elaborated in RDesigner software.



*Fig. 3.11. Optimal building orientation of implant on SLM platform and its support structures generated; Lattice unit of support structure  $x=y=z=1.0$  mm*

### 3.4. Configure the SLM process parameters

Setup the thickness of a layer powder (typically  $50 \mu\text{m}$ ) and slice the model. By default, RDesigner saves build jobs in its own REA material file. In addition to the slice data and generated build paths for laser tracks, this REA file contains all the SLM process parameters (laser power, scanning speed, hatch distance, etc.). To configure the SLM process parameters,

This project has been funded with support from the European Commission. This publication [communication] reflects the views only of the authors, and the Commission cannot be held responsible for any use which may be made of the information contained therein.

REditor software is used. This software tool is useful to optimize the SLM parameters, to define the scanning strategy, to organize the laser scanning steps (e.g., first scan the Outer-boundary, after scan the hatch area, and in the end the inner-boundary). An example is shown in Figure 3.12 where different functions are included as following: Outer-boundary, Inner-boundary, Hatch in X and Y direction. Beside these functions, the parameters for lattice support structures can be configured in the following function: X and Y Support (see Figure 3.12). Each function should be configured, and the main parameters can vary between:

- Laser power (10-200 W), expressed in mA where 5000 mA = 200 W;
- Scanning speed (100-2000 mm/s), expressed by Exposure Time and Point Distance;  
Example: Scanning speed 357 mm/s with Exposure Time 140  $\mu$ s and Point Distance 50  $\mu$ m (see Figure 3.12).

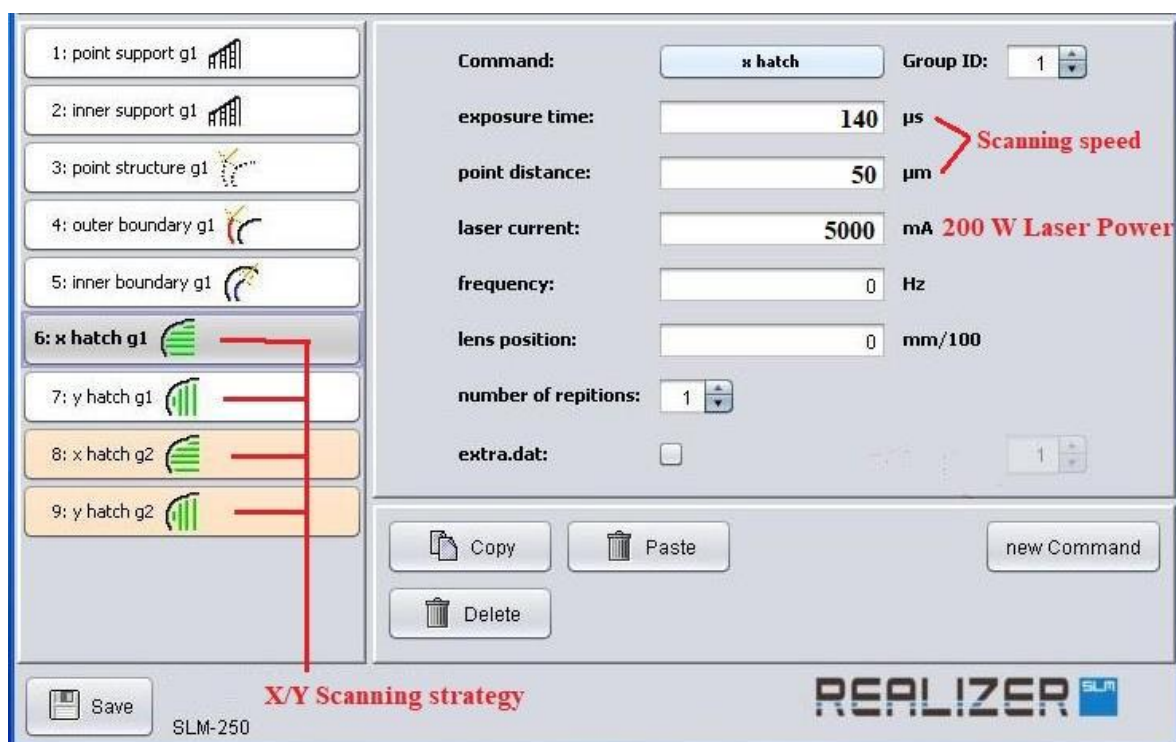
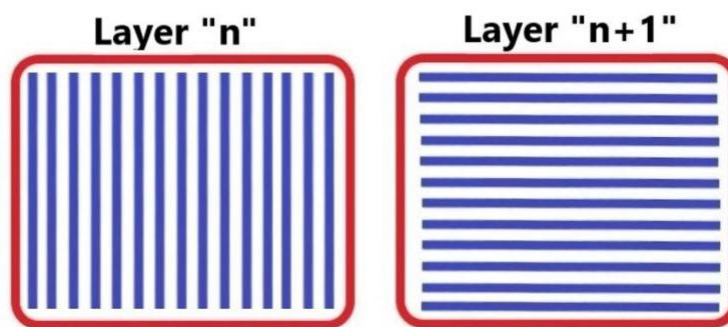


Fig. 3.12. Configure the SLM process parameters in REditor software

Moreover, the laser scanning strategy is another important aspect. Usually, we used an alternating X/Y strategy which allows a scanning in X direction of “n” layer and in Y direction of “n + 1” layer (rotating each hatch scan 90°) [Cosma’2020]. An example is shown in Figure 3.13. The advantage of this hatch pattern is that it can contribute to a high build rate compared with stripe hatch or chessboard pattern. On the other side, this scanning strategy can cause a rise of residual stress phenomena compared to the chessboard hatch pattern, and a special attention must be given to process parameters.



*Fig. 3.13. X/Y alternating laser scanning strategies; Laser functions used to scan the part:  
Outer-boundary – Red, Hatch area – Blue [Cosma’2020]*

To summary this step, the main SLM parameters for Ti implant will be:

- Slice thickness 50  $\mu\text{m}$ , resulting 466 slices;
- Scanning strategy X/Y;
- Hatch area 120 laser power and 357 scanning speed;
- Outer-boundary area 120 laser power and 500 mm/s scanning speed;
- Inner-boundary area 120 laser power and 500 mm/s scanning speed;
- Support structures 120 laser power and 750 mm/s scanning speed.

These SLM parameters were tested previously and conduct to a stable processability without technological defects.

### 3.5 SLM simulation

Since the cost of SLM fabrication is high, simulations are often used to predict the behavior of the part during processing. Using created REA file of the SLM job, manufacturing simulation can be elaborated. Figure 3.14 shows a simulation of SLM manufacturing in RDesigner at different slices.

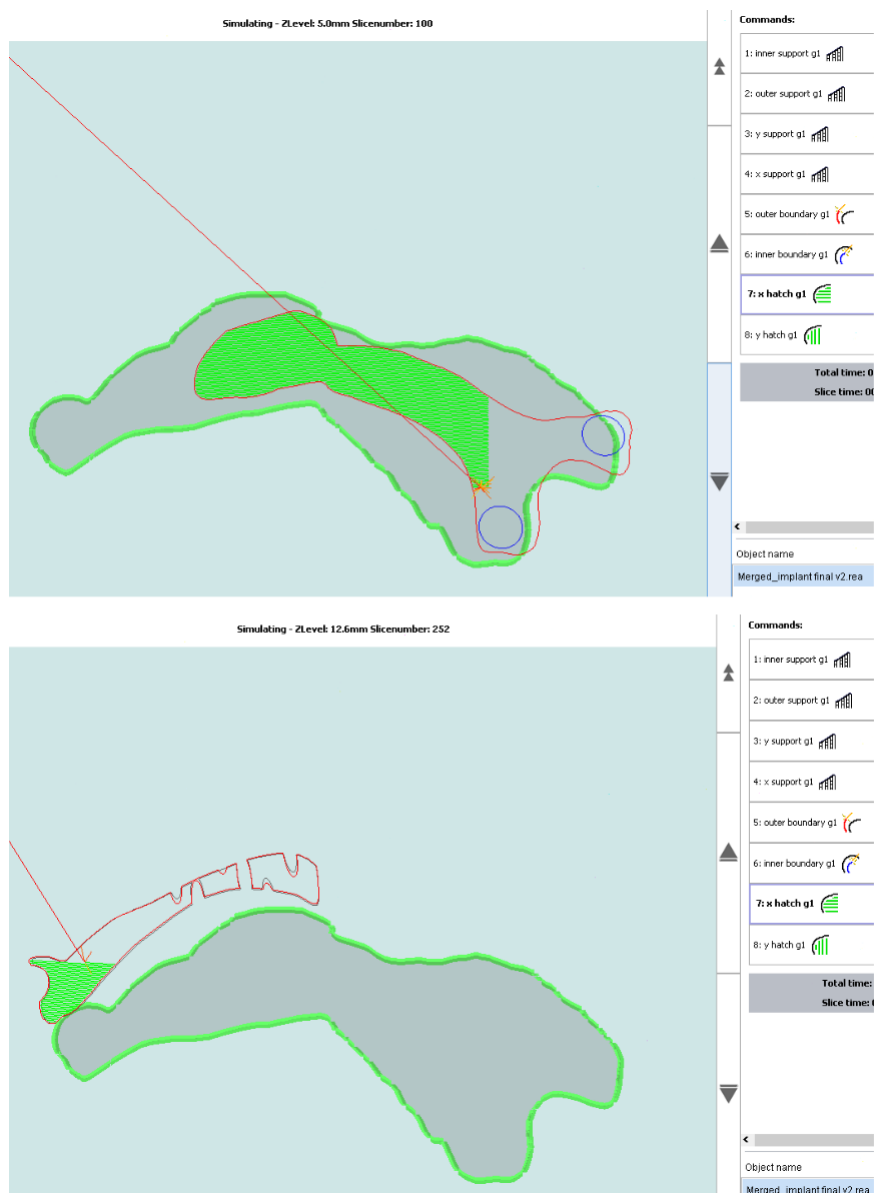


Fig. 3.14. SLM simulations at 100 and 252 slices

This project has been funded with support from the European Commission. This publication [communication] reflects the views only of the authors, and the Commission cannot be held responsible for any use which may be made of the information contained therein.

Figure 3.15 shows a zoom capture of SLM simulation at slice 100 and 101 respectively. Here it can be seen the effect of X/Y laser scanning strategy. At layer 100, the laser scans the section in X direction, and the next layer is scanned in Y direction.



Fig. 3.15. SLM simulations at 100 and 101 slices

### 3.6 Estimation of production time and cost

Figure 3.16 shows an estimation of manufacturing costs using RCalculator tool. Importing the REA file with all the SLM parameters and implant slices, this app calculates the production cost (448 €) and time to fabricate it (6.36 h). Regarding the production costs, they vary between 50 € to 80 € per hour being influenced by multiple factors as material, part complexity, etc. Post-processing procedures will add supplementary fees for stress relief treatment, support removal, finish/polishing, CNC machining, and surface treatments.

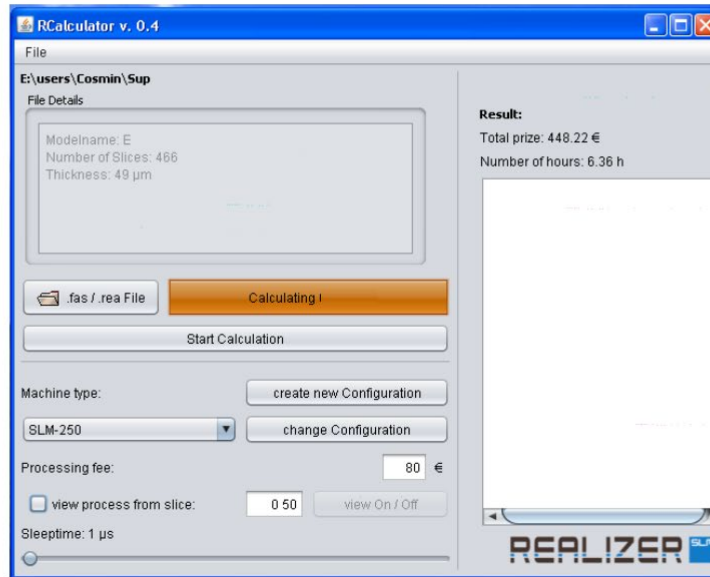


Fig. 3.16. Production cost and time to manufacture the designed Ti implant, RCalculator software

### 3.7 SLM-manufacturing of implant

Figure 3.17a shows how the Realizer machine is prepared, more exactly the base plate is calibrated to reference level. The platform should be brought in the right Z-height. This height can be controlled with a spatula. The steps are:

1. Raise platform by 0.10 mm and drive the recoater to the front and to the back.
2. Repeat till you can see the complete platform through the powder bed.
3. Press “Set Zero” for the elevator in Motors page to determine the actual position of the platform as zero position (Figure 3.18 b).

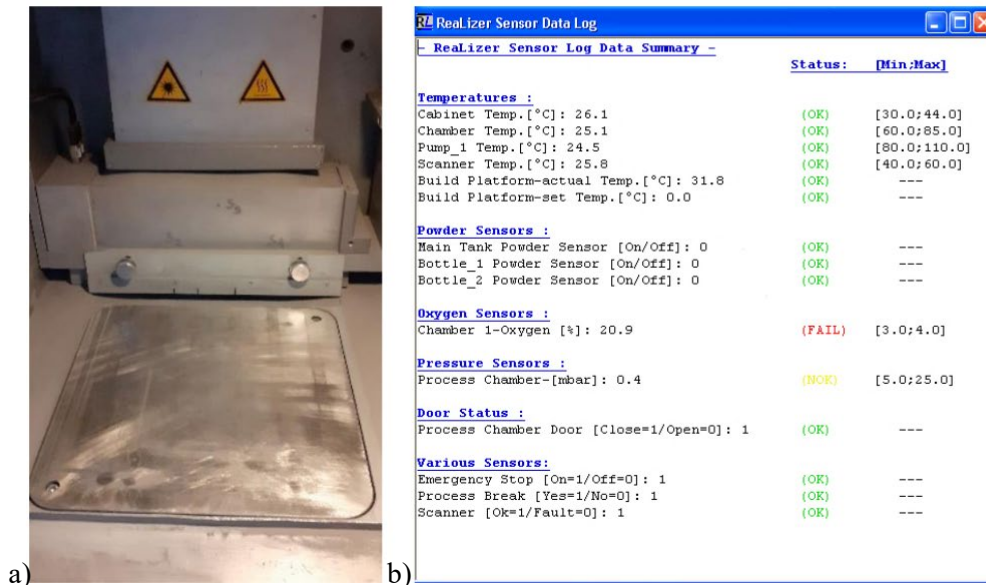


Fig. 3.17. a) Preparing the SLM base plate at reference level; b) Control all the machine sensor

To start the Realizer 250 machine, the following routine steps should be done in Realizer software [MCP]:

1. Control all the data from sensors (see Figure 3.17b) and clean the cover of the F-Theta lens with glasses wipes.
2. Close the build chamber and start flooding routine by pressing “Flood ON” in Motors page (Figure 3.18 b).
3. Turn the heating on if desired.
4. When the machine has reached an oxygen value lower than 1% (Figure 3.18 a) turn off the flooding routine by pressing “Flood OFF” in Motors page (Figure 3.18 b).
5. Turn on the gas pump by pressing “Gas pump on” (Figure 3.18 b) till you have reached an oxygen value of 0.2% (Figure 3.18 a).
6. If 0.2% or lower is reached turn of flooding routine (“flood off”) and press “Gas On”.
7. Now you must level the platform by driving the recoater to the front of the base plate, drop a little bit of powder by putting a value of 10.000 in the command box of the loader 2 in Motors page. Afterwards drive the recoater back to the end of the build chamber.
8. Import the REA file you want to fabricate.

This project has been funded with support from the European Commission. This publication [communication] reflects the views only of the authors, and the Commission cannot be held responsible for any use which may be made of the information contained therein.

9. Start the laser in Laser page (Figure 3.18 c).
10. Start the job by pressing the yellow “GO” in the Realizer software.
11. Then put in the slice you want to start from. First layer to be built is usually “0” and Press “OK”. *Now the machine starts the fabrication.* During the fabrication, the oxygen concentration should be lower than 2% in an argon protection gas.

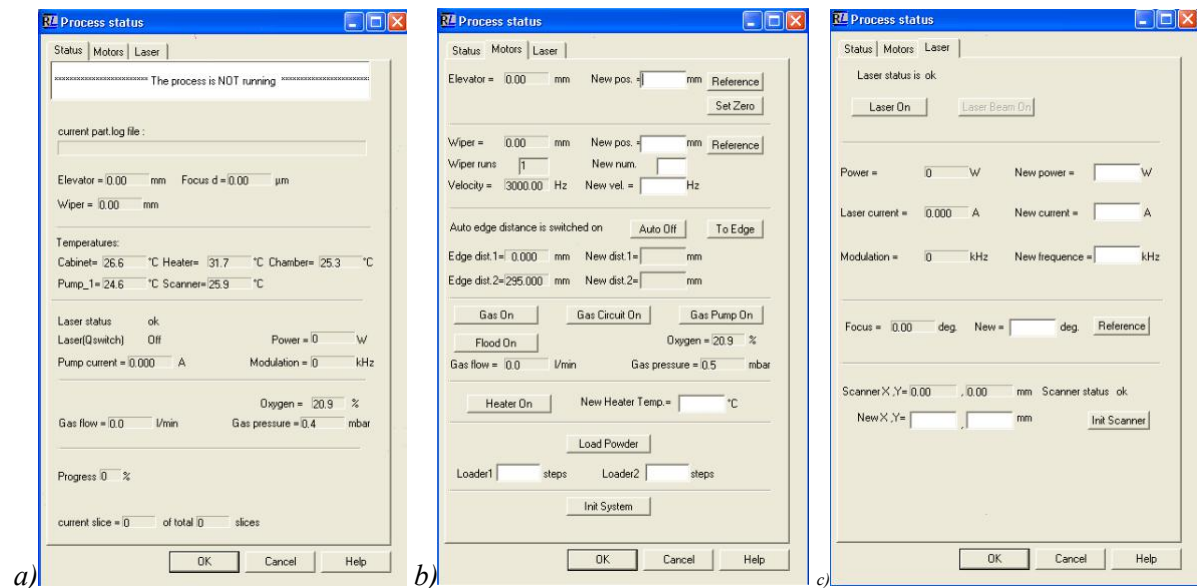


Fig. 3.18. Realizer software: a) Process status (wiper position, scanner/pump/cabinet/platform temperature, oxygen level, etc.); Technological parameters setting up: b) Motors page (temperature of base plate, on/off gas pump, elevator position); c) Laser page

Figure 3.19 shows some images during the SLM manufacturing at 258 slice. The SLM parameters and conditions conduct to proper fabrication without any unfavorable issues or defects. The production time was 6.51 h, being slightly longer than the theoretically estimated time in RCalculator tool (6.36 h - Section 3.6 Estimation of production time and cost).

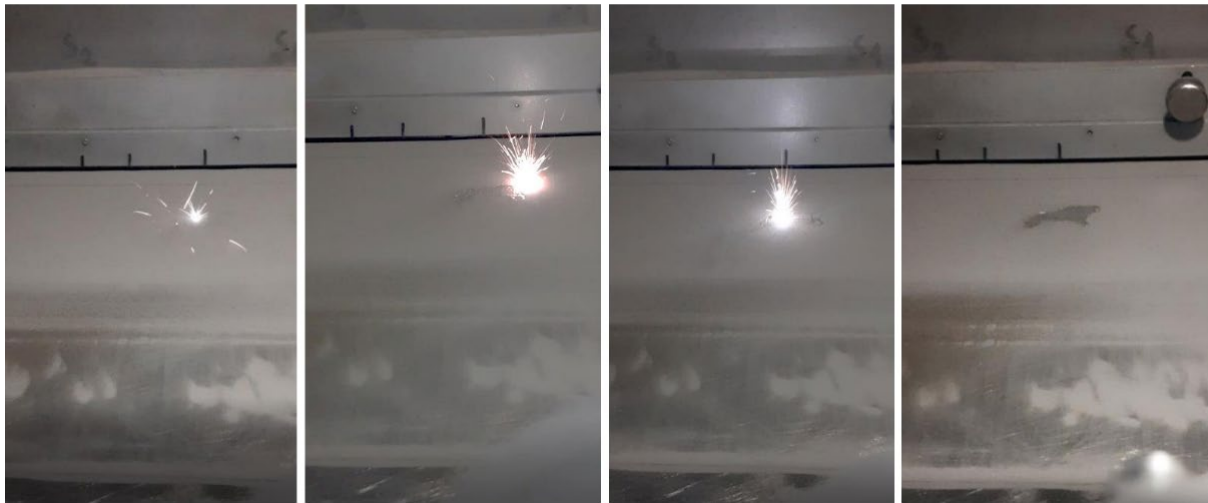


Fig. 3.19. SLM manufacturing of Ti implant

Figures 3.20-3.22 details some diagrams generated during the SLM fabrication of Ti implant. In general, the time needed to scan a powder layer varied between 25 s to 30 s being influenced by the area that needs to be irradiated by Nd:YAG laser. The laser power was maintained constant at 120 W for each scanning function. The build platform and working chamber recorded a temperature up to 44°C and 30°C respectively. The gas pressure was limited to 11.0-11.2 mbar. After the SLM machine scan the first 60 layers, the oxygen content decrease from 1.5% to 0.4% in an argon atmosphere.

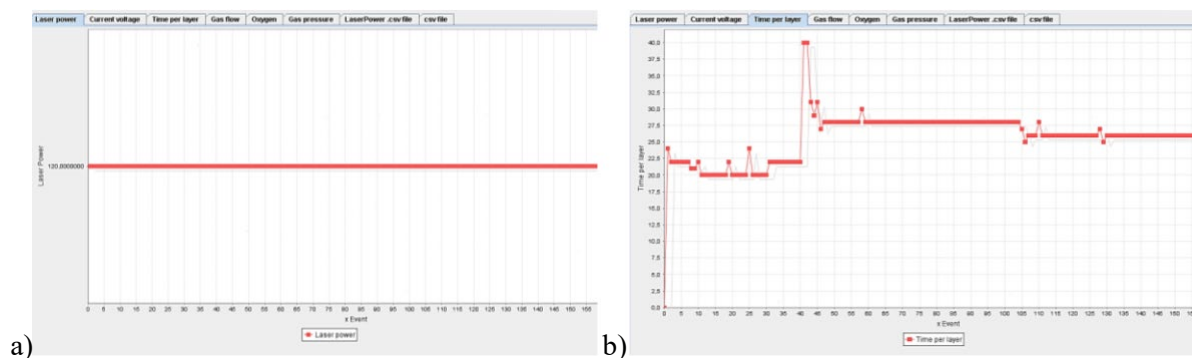


Fig. 3.20. Diagrams generated during the SLM fabrication by machine sensors:

a) Laser power, b) Time per each layer expressed in seconds

This project has been funded with support from the European Commission. This publication [communication] reflects the views only of the authors, and the Commission cannot be held responsible for any use which may be made of the information contained therein.

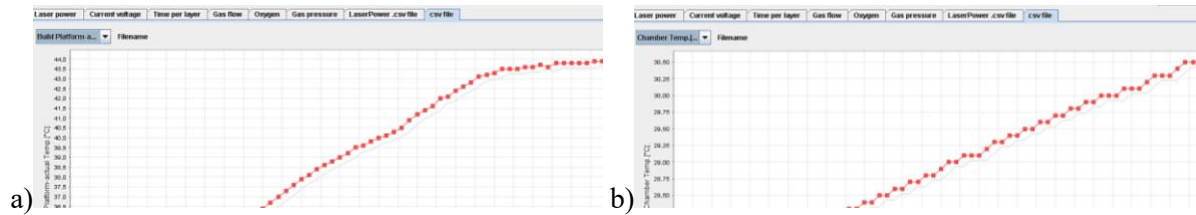


Fig. 3.21. Diagrams generated during the SLM fabrication by machine sensors: a) Build platform, b) Working chamber

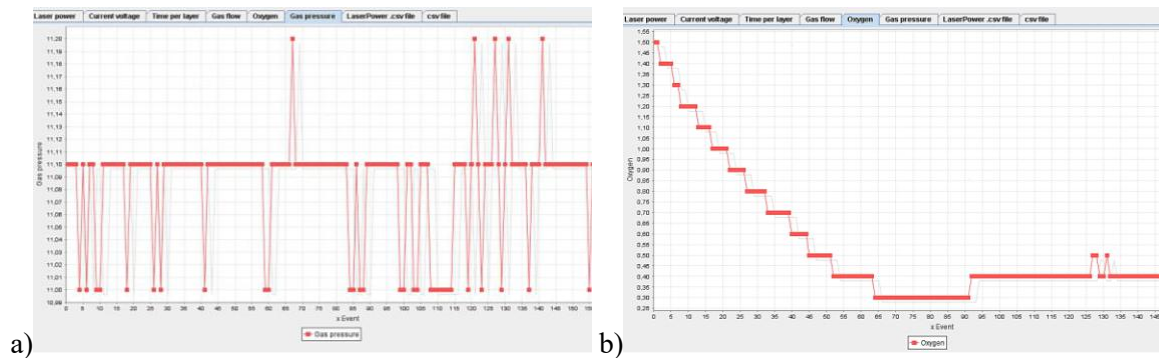


Fig. 3.22. Diagrams generated during the SLM fabrication from working chamber zone:

a) Gas pressure, b) Oxygen content

Figure 3.23 shows the step undertaken to clean the implant after SLM-manufacturing. Using a brush, the un-melted powder is removed and recycled for future works. To recycle the un-used powder, a vibratory sieve shaker is operated.



Fig. 3.23. Cleaning the implant of powder

This project has been funded with support from the European Commission. This publication [communication] reflects the views only of the authors, and the Commission cannot be held responsible for any use which may be made of the information contained therein.

To clean the anatomical surface of implant, a pneumatic biax tool can be used (biax compressed air angle grinder). The polishing of Ti implant is done with milling tools and carborundum abrasive discs mounted on a micro-motor at 10,000-15,000 rpm (Figure 3.24). The below image shows the implant with as-built surfaces and polished.



Fig. 3.24. Biax micro-motor used to polish the implant

This project has been funded with support from the European Commission. This publication [communication] reflects the views only of the authors, and the Commission cannot be held responsible for any use which may be made of the information contained therein.